Estimation of soils thermophysical characteristics in a nonlinear inverse heat transfer problem

Sultan Alpar, Julien Berger, Bolatbek Rysbaiuly, Rafik Belarbi

Estimation of soils thermophysical characteristics in a nonlinear inverse heat transfer problem

Sultan Alpar[a,b*], Julien Berger[a], Bolatbek Rysbaiuly[b], Rafik Belarbi[a]

[a] Laboratoire des Sciences de l'Ingénieur pour l'Environnement (LaSIE), UMR 7356 CNRS, La Rochelle Université, CNRS, 17000, La Rochelle, France

[b] International Information Technology University (IITU), 34/1 Manas street, 050040, Almaty, Kazakhstan

*corresponding author, e-mail address : sultan.alpar@univ-lr.fr, s.alpar@iitu.edu.kz

Abstract

It is well known that knowledge of thermophysical parameters is a leading strategy to research effects of energy transfer in soils. The present article proposes an inverse analysis for numerical solving of nonlinear heat transfer problem to determine the thermophysical properties of two different soil types: sand and chernozem. First, estimation of thermophysical parameters is performed using temperature data from experimental set-up, which is two-chambered container for two soil types. Second, numerical algorithm is based on implicit Euler scheme for discretization, Newton method to solve nonlinear system of equations and Levenberg-Marquardt method to minimize nonlinear estimator with Tikhonov's regularization technique. Simulations have been efficiently carried out for two different soil types, showing that the reliability of the model is satisfying with a discrepancy between numerical predictions and experimental observations remaining within the measurement error.

Key words: inverse problem, heat transfer, thermophysical properties, soil, Levenberg-Marquardt method

Nomenclature

T	temperature, $[\mathsf{K}]$	T_∞^L	ambient temperature on the left boundary, $[\mathsf{K}]$
x	horizontal space coordinate , $[\mathsf{m}]$	T_∞^R	ambient temperature on the right boundary, $[\mathsf{K}]$
L	total length of the container , $[\mathsf{m}]$	$\boldsymbol{P_m}$	vector of coefficients , $[-]$
ξ	position of the contact surface , $[\mathsf{m}]$	$\boldsymbol{Y}$	vector of measurements , $[\mathsf{K}]$
t_f	total duration of the experiment , $[\mathsf{h}]$	$\boldsymbol{T(P_m)}$	vector of numerical solutions, $[\mathsf{K}]$
k	heat conductivity , $[\mathsf{W.m^{-1}.K^{-1}}]$	J	sensitivity matrix, $[-]$
c_m	specific heat capacity , $[\mathsf{J \cdot kg^{-1} \cdot K^{-1}}]$	σ_T	total uncertainty, $[\mathsf{K}]$
ρ_m	material density , $[\mathsf{kg \cdot m^{-3}}]$		
h_m	heat transfer coefficient , $[\mathsf{W \cdot m^{-2} \cdot K^{-1}}]$		

1 Introduction

Soil thermophysical characteristics play main role in land surface processes modeling due to great effect on a vast range of chemical, physical and biological processes for energy distribution at multiple soil layers. Thermophysical properties determine the movement of heat in soils and influence how energy is partitioned in the soil profile. The knowledge of these quantities is crucial in different branches of engineering, environmental and earth science disciplines and most importantly for energy balance impact. The use and capabilities of energy geostructures in the context of both soil source heat pump systems and underground thermal energy storage systems (UTES) are addressed in [1]. The UTES often used for integration with a nuclear power plant. The success of the UTES is largely dependent on surrounding soil conditions [2]. In the work of [3] the thermal influence of the water filled pipe to the soil excess of 4 m during 4 months period [3]. This fact leads to suggestion that geothermal heat flow and heat loss determinations from buried pipelines and cables need careful consideration of environmental interactions. In [4], authors highlight the importance of high thermal conduction characteristic of soil for radioactive waste

disposal at great depth. In [5], authors describes cases when fluctuations in soil temperature, thermal diffusivity and ground heat flux are used as earthquake precursors. LUNT *et al.* proposed improvements for building thermal performance by choosing artificial soils with different thermal conductivity properties [6]. Last, the soil thermal conductivity is always viewed as one of the most important thermophysical characteristics because of the impact on the soil heat balance [7, 8]. All these research illustrate the necessity of knowing precisely soil thermal physical properties

Precise estimation of soil thermophysical properties is always arduous due to the direct *in-situ* measurement difficulties, impact of density [9], porosity and interactions with moisture [10–12]. In spite of progress made in techniques for soil heat flux measurement, direct measurement still remains relatively expensive, destructive, labour intensive, time consuming and impractical for large scale applications or computer simulations due to space and time variability in parameters. Therefore, thermal properties are often estimated by solving inverse heat transfer problem. Such procedure aims at retrieving the properties that minimizes the difference between the mathematical model predictions and temperature measurement data obtained at different depths in the soil. Mathematically speaking, the inverse heat transfer problems are ill-posed. Since problem is ill-posed, specific attention to the choice of the inverse problem method should be made [13, 14].

Despite possible mathematical proofs of solution existence and uniqueness, inverse problem are very sensitive to error in the measured input data. Thus, the solution of an inverse problem requires special stabilization techniques, commonly known as regularization methods. In fact, the ill-posed inverse problem is not really solved, but an approximate solution is obtained based on an approximate well-posed regularized problem. A. N. TIKHONOV introduced a pioneering approach to problem-solving, particularly highlighted in [15]. He was the first mathematician to articulate a comprehensive methodology that relied on the creation of specialized algorithms known as regularizing operators. Building upon this theoretical framework, A. N. TIKHONOV put forth the Variational Regularization Method, incorporating a numerically small parameter. This theoretical approach has since gained widespread adoption in numerous practical research in the world. Subsequently, in [16], this overarching method served as a foundation for the advancement of diverse approaches and algorithms, including those employed in various iterative methods. Which lead to ALIFANOV's new method - iterative regularization technique, based on gradient methods first proposed and justified in [17–19]. The notable aspect of this approach is that it eliminates the need for an extra regularization parameter. Instead, the iteration number itself assumes this role directly. This assertion holds true for nearly all gradient algorithms, including the highly effective conjugate gradient method with its superlinear convergence rate. Adopting the iterative regularizatrion method another approach to solve ill-posed heat transfer problem created - BECK's sequential technique, where regularization is obtained from the averaging properties of least squares and from the measurements taken at future time steps [20]. Similarly more recently, stochastic simulation techniques are becoming very popular for the solution of inverse problems [21]. These simulation techniques generate samples of a statistical distribution and inference on the distribution is obtained through inference on the samples. A very common approach for the solution of inverse problems, dealing with the estimation of the parameters $\boldsymbol{P}$ with the measurements $\boldsymbol{Y}$, is to find a point estimate that maximizes *the likelihood probability density*. This can be accomplished through the minimization of *the maximum likelihood objective function*. There are plenty of minimization methods. In [22–24], authors use Conjugate Gradient method (CGM) with adjoint problem for the thermal contact conductance and source parameter determination, which is given as function with the noise. In contrast, advantage of the work [25] is that it uses CGM without involvement an adjoint problem, but the method still requires calculation of the gradient direction coefficient and a search step length. In order to avoid this downside LEVENBERG-MARQUARDT method can be used, which allows automatic control of the damping parameter. Method were successfully used in several researches [26–29] for heat and mass transfer problems. The main drawbacks of these works are

use of synthetic data for measurements and application of finite difference approach for sensitivity analysis, which leads to additional computational costs to achieve desired approximation order.

The aim of this work is to determine the thermophysical properties of two different soil types, which are sand and chernozem. In this research, we propose inverse analysis for numerical solving of nonlinear heat transfer problem. The algorithm is based on the backward EULER time advancement scheme for the direct problem solution and LEVENBERG-MARQUARDT iterative algorithm to minimize the least square estimator with TIKHONNOV's regularization, which modifies objective function by the addition of a penalty term. The LEVENBERG-MARQUARDT method is the combination of the steepest-descent and GAUSS-NEWTON methods. Estimation of thermophysical parameters is performed using the temperature data obtained from experimental set-up and computation of the sensitivity coefficients by direct differentiation of the governing equations. In addition, the discrepancy principle is used to stop iterative procedure for LEVENBERG-MARQUARDT method. Experimental set-up is two-chambered container for two soil types. Experimental observations help us solve the parameter estimation problem and evaluate the reliability of the calibrated model. First set of experimental data is used for estimation of parameters. Another set is used for comparison of numerical results to experimental data which leads to the robustness of analysis.

The paper is organized as follows. Section 2 presents the governing equation with boundary conditions. It follows with the description of the LEVENBERG-MARQUARDT method, with the presentation of the initial boundary problems to determination of sensitivity coefficients and with the general strategy to solve nonlinear inverse problem used in article. Then, in section 3 numerical problem is described. The NEWTON method is used to solve direct nonlinear heat transfer problem. In section 4 the experimental set-up is detailed with description of total uncertainty of the observations. Finally, the section 5 presents estimated parameters, sensitivity coefficients.

2 Mathematical model

The problem involves heat transfer through the constructed two-chamber container filled with the two types of soil. Figure 1 schematically shows the container. The side faces are thermally insulated while the lateral ones are in contact with the environment (air). Thus, the transfer is assumed as one dimensional.

2.1 Governing equations

The one-dimensional nonlinear heat diffusion transfer equation is considered in a two layer container with different soils. The physical process are observed for the time domain $\Omega_t : t \in [0,\, t_f]$, where $t_f \left[\,\mathsf{h}\,\right]$ is the total duration of the experiment. The space interval $\Omega_x : x \in [0,\, L]$ is illustrated in Figure 1, where $L \left[\,\mathsf{m}\,\right]$ and $\xi \left[\,\mathsf{m}\,\right]$ are total length of the two-chamber container and position of the contact surface, respectively. The temperature is defined as:

$$T\colon [0,\, L] \times [0,\, t_f] \to \mathbb{R}. \tag{1}$$

The governing nonlinear equation of heat diffusion transfer is:

$$c_m\left(T\right) \rho_m\left(T\right) \frac{\partial T}{\partial t} = \frac{\partial}{\partial x}\left(k_m\left(T\right) \frac{\partial T}{\partial x}\right), \tag{2}$$

where $c_m \left[\,\mathsf{J}\cdot\mathsf{kg}^{-1}\cdot\mathsf{K}^{-1}\,\right]$ is the specific heat capacity, $\rho_m \left[\,\mathsf{kg}\cdot\mathsf{m}^{-3}\,\right]$ is the material density and $k_m \left[\,\mathsf{W}\cdot\mathsf{m}^{-1}\cdot\mathsf{K}^{-1}\,\right]$ is the thermal conductivity, index $m = 1,\, 2$ shows the type of the material, $1-$sand, $2-$black soil, respectively . If the thermophysical properties may be assumed as constant

as first order hypothesis, it is assumed here that these coefficients vary with temperature. The following temperature dependencies are used:

$$\begin{aligned} c_m\left(T\right) &= c_{m,0} + c_{m,1}T, \\ \rho_m\left(T\right) &= \rho_{m,0} + \rho_{m,1}T, \\ k_m\left(T\right) &= \ k_{m,0} + k_{m,1}T + k_{m,2}T^2 + k_{m,3}T^3. \end{aligned} \tag{3}$$

The initial conditions of the problem is computed considering a linear interpolation between the measured temperatures and considered as a function of space:

$$T\left(x, t=0\right) = T_0\left(x\right) \tag{4}$$

On the front side and end side surfaces of the container, a FOURIER/ROBIN boundary condition is assumed:

$$\begin{aligned} \left(k_m\left(T\right)\frac{\partial T}{\partial x}\right)\Big|_{x=0\,,\,t} &= \left(h_m\left(T\right)\left(T - T_\infty^L\left(t\right)\right)\right)\Big|_{x=0\,,\,t}, \\ \left(k_m\left(T\right)\frac{\partial T}{\partial x}\right)\Big|_{x=L\,,\,t} &= \left(-h_m\left(T\right)\left(T - T_\infty^R\left(t\right)\right)\right)\Big|_{x=L\,,\,t}, \end{aligned} \tag{5}$$

where $T_\infty^L\left(t\right)$ and $T_\infty^R\left(t\right)$ are ambient temperatures, $h_m\left[\mathsf{W}\cdot\mathsf{m}^{-2}\cdot\mathsf{K}^{-1}\right]$ is heat transfer coefficient, which is also function of a temperature depends on the type of the material:

$$h_m\left(T\right) = \ h_{m,0} + h_{m,1}T \tag{6}$$

Assuming the surface between two layers in perfect contact, continuity conditions on the temperature and the heat flux are expressed as follows:

$$\begin{aligned} T(\xi\epsilon\,,\,t) \ &= \ T(\xi \ + \ \epsilon\,,\,t)\,, \\ \left(k_m(T)\frac{\partial T}{\partial x}\right)\Big|_{\xi-\epsilon\,,\,t} \ &= \ \left(k_m(T)\frac{\partial T}{\partial x}\right)\Big|_{\xi+\epsilon\,,\,t}, \quad \epsilon \to 0\,. \end{aligned} \tag{7}$$

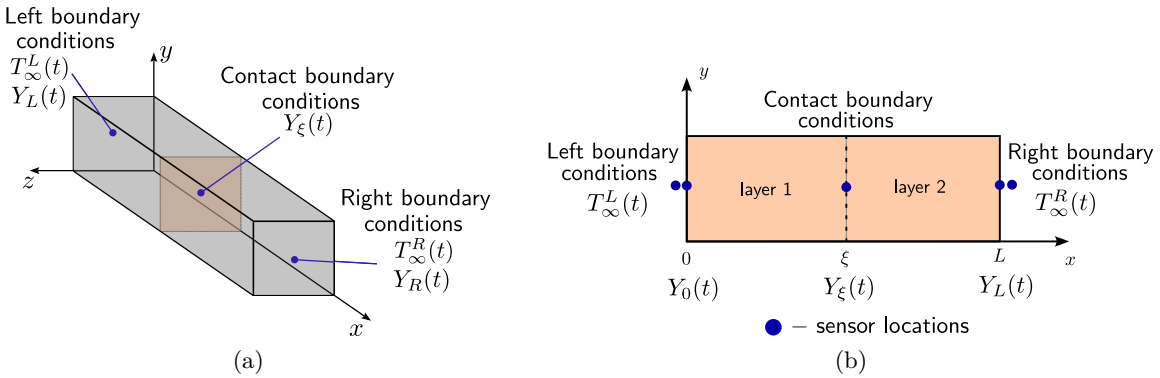

Figure 1. *Experimental set-up illustration with appropriate boundary conditions position (a), scheme of the sensor locations along the container (b).*

2.2 Nonlinear inverse problem

For the nonlinear inverse problem considered of interest in our research, the temperature-varying thermophysical properties of the soil are regarded as unknown. The additional experimental data obtained from transient temperature measurements $Y_{x^*}^n$ at times t_n , $n \in \{1, 2, \ldots, N_t\}$

and at the locations $x^* = 0$, ξ, L are used for the estimation of the coefficients defining the functions $k_m(T)$, $c_m(T)$, $\rho_m(T)$ and $h_m(T)$. Given equations (3) and (6), a total of 20 coefficients are unknown:

$$\boldsymbol{P_m} = (k_{m,0},\, k_{m,1},\, k_{m,2},\, k_{m,3},\, c_{m,0},\, c_{m,1},\, \rho_{m,0},\, \rho_{m,1},\, h_{m,0},\, h_{m,1}),\; m = 1,\, 2. \tag{8}$$

The measurement errors, $\boldsymbol{\varepsilon}$, are assumed to be additive, which are Gaussian errors with zero means:

$$\boldsymbol{Y} = \boldsymbol{T(P_m)} + \boldsymbol{\varepsilon}. \tag{9}$$

where $\boldsymbol{T(P)}$ is the solution of the mathematical formulation (2), obtained with the vector of parameters $\boldsymbol{P_m}$, that is:

$$\boldsymbol{T}^t = [T_1(\boldsymbol{P_m}), T_2(\boldsymbol{P_m}), \ldots, T_{N_t}(\boldsymbol{P_m})]. \tag{10}$$

It is assumed that measurements are uncorrelated with the constant variance. Thus, the estimation of 20 unknown parameters, $\boldsymbol{P_m} = (p_{m,j})$, $j = 1, \ldots, 10$, $m = 1,\, 2$ (e.g. $p_{2,5} = c_{2,0}$), can be achieved by the minimization of the following cost function, which is in our case ordinary least squares norm with addition of Tikhonov's regularization:

$$S_{OLS}\,(\boldsymbol{P_m}) \;=\; [\boldsymbol{Y} - \boldsymbol{T(P_m)}]^t\,[\boldsymbol{Y} - \boldsymbol{T(P_m)}] \;+\; \alpha\,[\boldsymbol{P}_{prior} - \boldsymbol{P}]^t\,[\boldsymbol{P}_{prior} - \boldsymbol{P}] \tag{11}$$

Here, α is the regularization parameter. The values chosen for the regularization parameter α influence the stability of the solution as the minimization is performed. For $\alpha \to 0$, exact matching between estimated and measured temperatures is obtained with the minimization of $S_{OLS}\,(\boldsymbol{P_m})$ and the inverse problem solution becomes unstable because of its ill-posed nature. On the other hand, for large valuse of α, when the second term in Eq. (11) is dominant, the parameters $\boldsymbol{P}$ tend to become constant. Therefore, instabilities on the solution can be alleviated by proper selection of the value of α. Tikhonov [16] recommended that α should be selected so that the minimum value of the first term of the objective function would be equal to the sum of the squares of the errors expected for the measurements, which is known as Morozov's discrepancy principle [30]. Also, the use of so-called L-curve [14] appears as a useful technique for the selection of the regularization parameter. Since the norms of the solution and the residual is important, it is natural to plot these two quantities versus each other as a curve:

$$\Big(\,\|\,\boldsymbol{Y} - \boldsymbol{T(P_m)}\,\|_2\,,\; \|\,\boldsymbol{P}_{prior} - \boldsymbol{P}\,\|_2\,\Big) \tag{12}$$

This is L-curve, which is illustrated in Figure 2 for both types of soils.

To minimize the objective function (11) the Levenberg-Marquardt method is used. This technique uses both Gauss-Newton and steepest descent approaches to converge to an optimal solution.

$$\boldsymbol{P}^{\star}:\; \stackrel{def}{=} \arg\,\min\; S_{OLS}\,(\boldsymbol{P_m}) \tag{13}$$

For the simplicity in the explanation, derivation are first performed here by considering measurements of one single sensor:

$$\boldsymbol{Y}^t = [Y_0, Y_1, \ldots, Y_{N_t}] \tag{14}$$

To minimize the objective function (11), we need to equate to zero the derivatives of $S_{OLS}\,(P)$ with respect to each of the unknown parameters $p_{m,j}$.

$$\boldsymbol{\nabla} S_{OLS}\,(\boldsymbol{P_m}) = -2J^T[\boldsymbol{Y} - \boldsymbol{T(P_m)}] \;-\; 2\alpha\,[\boldsymbol{P}_{prior} - \boldsymbol{P}] = 0 \tag{15}$$

where J is the sensitivity matrix:

$$J = \left[\frac{\partial \boldsymbol{T}^T\,(\boldsymbol{P_m})}{\partial \boldsymbol{P_m}}\right]^T = 0 \tag{16}$$

Due to nonlinearity of inverse problem, the sensitivity matrix has some functional dependence on the vector of unknown parameters $\boldsymbol{P_m}$. The solution then requires an iterative procedure, which is obtained by using a TAYLOR series expansion around current solution $\boldsymbol{P_m^s}$ at iteration s for the vector of estimated temperatures $\boldsymbol{T(P_m)}$:

$$\boldsymbol{T(P_m)} \approx \boldsymbol{T(P_m^s)} + J^s \left(\boldsymbol{P_m} - \boldsymbol{P_m^s}\right) \tag{17}$$

where $\boldsymbol{T(P_m^s)}$ and J^s are the estimated temperature and the sensitivity matrix calculated at iteration s. To obtain the vector of unknown parameters $\boldsymbol{P_m}$, equation (17) is substituted in (15). After algebraic rearrangements the following iterative equation is derived to obtain the vector of unknown parameters $\boldsymbol{P_m}$:

$$\boldsymbol{P_m^{s+1}} = \boldsymbol{P_m^s} + \left[J^T J \ + \ \alpha \, \boldsymbol{I}\right]^{-1} \left[J^T (\boldsymbol{Y} - \boldsymbol{T(P_m^s)}) \ + \ \alpha \left[\boldsymbol{P}_{prior} - \boldsymbol{P}\right]\right] \tag{18}$$

where $\boldsymbol{I}$ is the identity matrix. The iterative procedure given by (18) is called the GAUSS method. Such method is actually an approximation for the NEWTON-RAPHSON method. We should note that the identifiability condition has to be satisfied to use (18), which is:

$$|J^T J| \neq 0 \tag{19}$$

The following criteria were used to stop the iterative procedure:

$$S_{OLS}\left(\boldsymbol{P_m^{s+1}}\right) < \varepsilon \tag{20}$$

where ε is prescribed tolerance. The criterion given by (20) can be conveniently selected by using MOROZOV's dicrepancy principle. This principle relies on the fact that the expected minimum values of the objective function (11) is obtained when the differences between measured and estimated temperatures are of the same order of magnitude of the measurement errors. The tolerance ε based on MOROZOV's discrepancy principle is thus obtained by assuming:

$$|\boldsymbol{Y^n} - \boldsymbol{T^n(P_m^{s+1})}| \approx \sigma^n, \tag{21}$$

where σ^n is the standard deviation of the measurement error at time t_n. If the measurements are uncorrelated and with a constant standard deviation, i.e. $\sigma^n = \sigma = constant$, we can substitute equation (21) into equation (11), which consequently gives us:

$$S_{OLS}\left(\boldsymbol{P_m^{s+1}}\right) < N_t \sigma^2 \tag{22}$$

2.3 Sensitivity coefficients

For the determination of the sensitivity coefficients involved in the computation of the sensitivity matrix (16), an initial-boundary value problem is developed for each parameter by differentiating the original direct problem (2) - (6) with respect to the unknown coefficients.

$$\theta_{m,j} = \frac{\partial T}{\partial p_{m,j}}, j = 1, \ldots, 10, \; m = 1, \, 2. \tag{23}$$

In our case we obtain 20 sensitivity equations for all the unknown parameters, but for the sake of simplicity let us write them for governing equation in general form:

$$c_m\left(T\right) \rho_m\left(T\right) \frac{\partial \theta_{m,j}}{\partial t} = \frac{\partial}{\partial x}\left(k_m\left(T\right) \frac{\partial \theta_{m,j}}{\partial x}\right) + F\left(\theta_{m,j}, T\right), \tag{24}$$

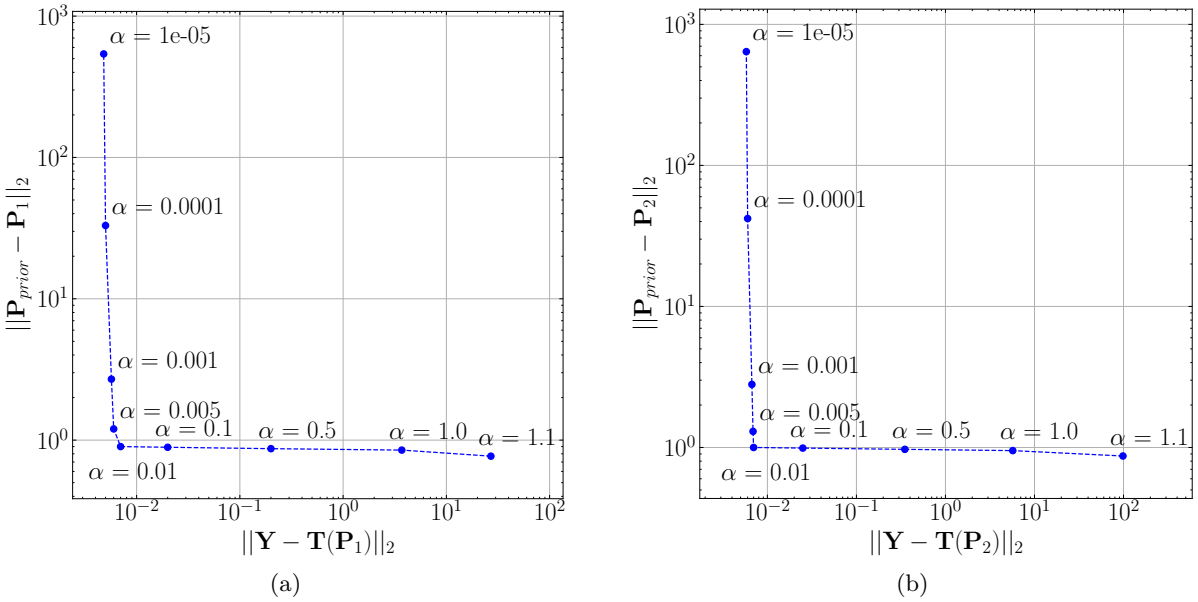

Figure 2. *L-curve for standard-form Tikhonov regularization for the first material (a) and the second material (b).*

where $F\left(\theta_{m,j}, T\right)$ is expressed as follows:

$$F\left(\theta_{m,j}, T\right) = -\frac{\partial c_m\left(T\right)}{\partial p_{m,j}} \rho_m\left(T\right) \frac{\partial T}{\partial t} - \frac{\partial \rho_m\left(T\right)}{\partial p_{m,j}} c_m\left(T\right) \frac{\partial T}{\partial t} + \frac{\partial}{\partial x}\left(\frac{\partial k_m\left(T\right)}{\partial p_{m,j}} \frac{\partial T}{\partial x}\right), \tag{25}$$

with initial condition:

$$\theta_{m,j}\left(x, t=0\right) = 0 \tag{26}$$

In case of boundary conditions, we get next conditions for sensitivity problem. Good way of presenting them in a synthetic way:

$$\begin{aligned}
\left(k_m\left(T\right) \frac{\partial \theta_{m,j}}{\partial x}\right)\Big|_{x=0\,,\,t} &= \left(h_m\left(T\right) \theta_{m,j} + \frac{\partial h_m\left(T\right)}{\partial p_{m,j}} \left(T - T_\infty^L\left(t\right)\right) - \frac{\partial k_m\left(T\right)}{\partial p_{m,j}} \frac{\partial T}{\partial x}\right)\Big|_{x=0\,,\,t}, \\
\left(k_m\left(T\right) \frac{\partial \theta_{m,j}}{\partial x}\right)\Big|_{x=L\,,\,t} &= \left(-h_m\left(T\right) \theta_{m,j} - \frac{\partial h_m\left(T\right)}{\partial p_{m,j}} \left(T - T_\infty^R\left(t\right)\right) - \frac{\partial k_m\left(T\right)}{\partial p_{m,j}} \frac{\partial T}{\partial x}\right)\Big|_{x=L\,,\,t},
\end{aligned} \tag{27}$$

where derivatives of the physical properties with respect to parameters can be easily obtained just following rules for differentiation. Firstly, system of equations (24) - (27) are discretized using backward Euler time advancement scheme. Secondly, obtained three-diagonal system of linear algebraic equations (SLAE) with unknown $\theta_{m,j}$ is solved using Thomas' method.

2.4 Strategy to solve IHTP

The strategy to solve the inverse heat transfer problem is to split into two subproblems Eqs. (2) - (7) according to each container. For both subproblems, the measurement data $Y_{x^*}^n$ from the sensor at $x^* = \xi$ is used as Dirichlet condition T_ξ. This is motivated by the following

First, it can be remarked that, estimation of thermophysical properties of both containers from the same measurement data is not possible. Indeed, the sensitivity coefficients would be linearly dependent, as will be demonstrated in Section 5 for the case study under investigations. For instance $k_{1\,,\,0}$ and $k_{2\,,\,0}$ have linearly dependent sensitivity coefficients. Then, for each

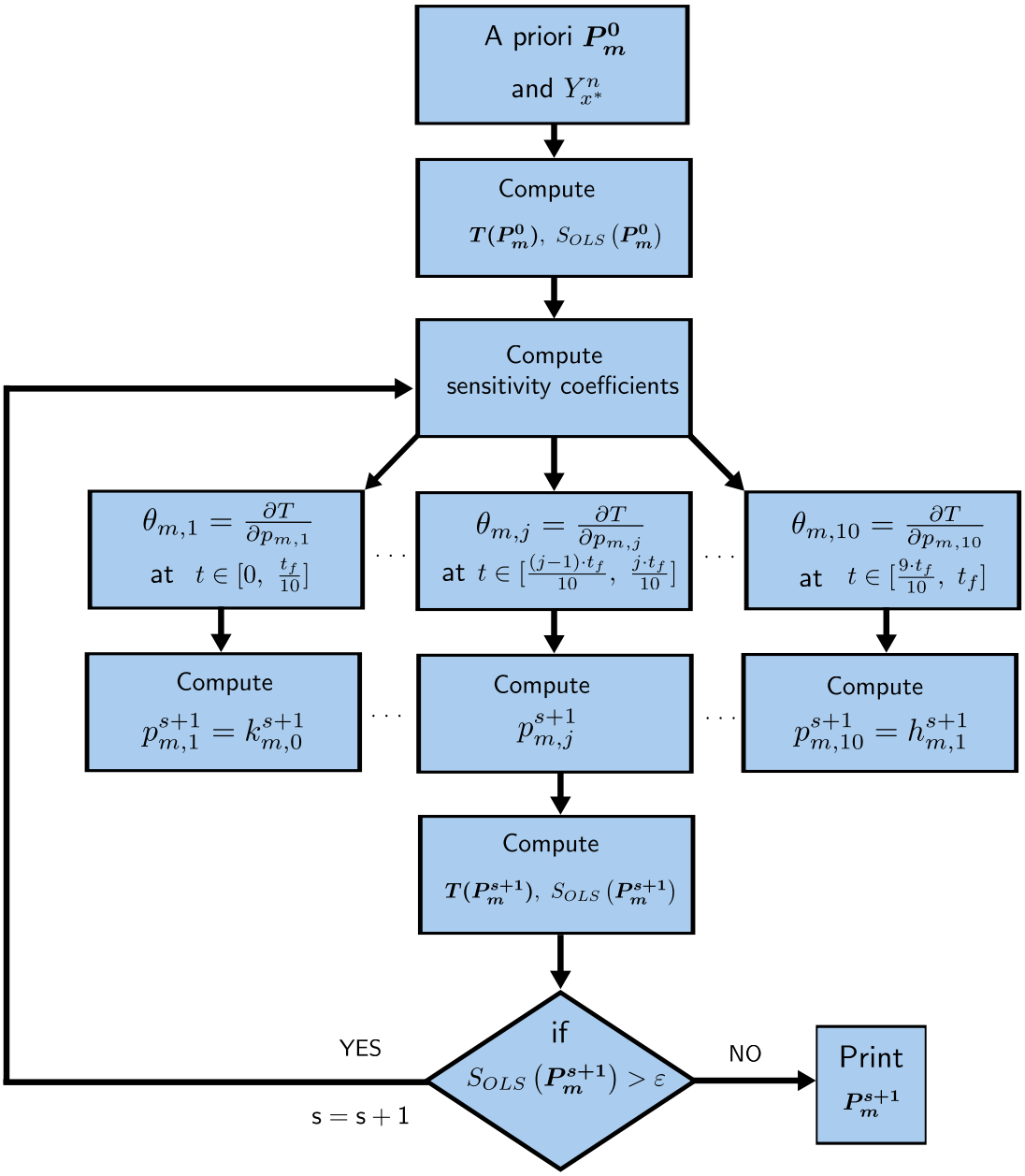

Figure 3. *Flow chart of parameter estimation algorithm*

container subproblem, some sensitivity coefficient can be linearly dependent as for instance $k_{1,0}$ and $c_{1,0}$ from Table 4. Thus, to satisfy condition (19), for each subproblem, the parameters are estimated in different time intervals. Namely, ten time intervals are considered for the first container denoted as $t \in [\frac{(j-1)\cdot t_f}{10}, \frac{j\cdot t_f}{10}]$, $j = \{1, \ldots, 10, \}$. Figure 3 shows schematically the procedure of estimation. For the sake of clarity the flow chart doesn't illustrate time intervals and measurement position for the all parameters.

In addition, the algorithm 1 presents the computational strategy based on the Levenberg-Marquardt method. Note that, the algorithm converges quite fast due to the explicit calculation of the damping parameter. Thus, the Levenberg-Marquardt method tends to the steepest descent method given by equation (18).

Algorithm 1 The computational algorithm for the proposed version of the Levenberg-Marquardt method.

Input: *a priori* estimates for parameters $\boldsymbol{P_m^{s=0}}$ and experimental data $Y_{x^*}^n$
Output: All thermophysical parameters after convergence of $S_{OLS}\left(\boldsymbol{P_m^s}\right)$
while $S_{OLS}\left(\boldsymbol{P_m^s}\right) > \varepsilon$ **do**
    Solve the direct problem given (2)-(5) using $\boldsymbol{P_m^s}$ to get $\boldsymbol{T(P_m^s)}$ at $t \in [0,\ t_f]$.
    for $j \leftarrow 1$ to 10 **do**
        Compute the sensitivity matrix by solving equations (24)-(27) to get $\theta_{m,j} = \frac{\partial T}{\partial p_{m,j}}$ at $t \in [\frac{(j-1)\cdot t_f}{10},\ \frac{j\cdot t_f}{10}],\ m = 1,\ 2,$
    Compute the new estimate $\boldsymbol{P_m^{s+1}}$ (18) for each time interval and sensor position.
    Calculate $S_{OLS}\left(\boldsymbol{P_m^{s+1}}\right)$ from Eq. (11).
    Replace s by $s+1$
end

3 Numerical problem

In order to describe numerical schemes a uniform discretization is used for space and time intervals $\Omega_x \rightsquigarrow \Omega_{h_x}$, $\Omega_t \rightsquigarrow \Omega_{h_t}$:

$$\Omega_{h_x} = \bigcup_{i=0}^{N_x} [x_i, x_{i+1}],\ x_{i+1} - x_i = \Delta x,\ \forall i \in \{1, 2, \ldots, N_x\}.$$

$$\Omega_{h_t} = \bigcup_{n=0}^{N_t} [t_n, t_{n+1}],\ t_{n+1} - t_n = \Delta t = const > 0,\ \forall n \in \{1, 2, \ldots, N_t\}.$$

The choice of the time and space step affects on the dicretization error. The values N_t and N_x are chosen according to the computational cost requirements. (x, t) coordinates on the plane intersect mesh/grid points/nodes. Thus the approximate solution of the direct problem is defined at the mesh nodes. The values of the $T(x,t)$ after discretization are written as $T_i^n := \overset{\text{def}}{} T(t_n, x_i)$.

First, problem (2) is discretized using the backward Euler time advancement scheme in combination with the second-order accurate centered finite difference formula:

$$\rho_m\left(T_i^{n+1}\right) c_m\left(T_i^{n+1}\right) \frac{T_i^{n+1} - T_i^n}{\Delta t} = \frac{1}{\Delta x}\left(k_m\left(T_{i+\frac{1}{2}}^{n+1}\right) \frac{T_{i+1}^{n+1} - T_i^{n+1}}{\Delta x} - k_m\left(T_{i-\frac{1}{2}}^{n+1}\right) \frac{T_i^{n+1} - T_{i-1}^{n+1}}{\Delta x}\right), \tag{28}$$

where $T_{i\pm\frac{1}{2}}^{n+1} = \frac{T_{i\pm1}^{n+1} + T_i^{n+1}}{2}$. In case of boundary and initial conditions we obtain next schemes:

$$\begin{aligned}
&t_0 = 0:\ T_i^0 = T_0\left(x_i\right), \\
&x_0 = 0:\ k_m\left(T_{\frac{1}{2}}^{n+1}\right) \frac{T_1^{n+1} - T_0^{n+1}}{\Delta x} = h_m\left(T_0^{n+1}\right)\left(T_0^{n+1} - T_\infty^{L,n+1}\right), \\
&x_{N_x} = L:\ k_m\left(T_{N_x-\frac{1}{2}}^{n+1}\right) \frac{T_{N_x}^{n+1} - T_{N_x-1}^{n+1}}{\Delta x} = -h_m\left(T_{N_x}^{n+1}\right)\left(T_{N_x}^{n+1} - T_\infty^{R,n+1}\right),
\end{aligned} \tag{29}$$

Due to the physical properties dependencies of temperature, we have nonlinearity. Thus to obtain solution we'll use iterative Newton's method, but before that let us rewrite the difference equation system (28) in the form:

$$F\left(T_{i+1}^{n+1}, T_i^{n+1}, T_{i-1}^{n+1}\right) \equiv \frac{\Delta t}{(\Delta x)^2} \cdot \left(k_m\left(T_{i+\frac{1}{2}}^{n+1}\right)\left(T_{i+1}^{n+1} - T_i^{n+1}\right) - k_m\left(T_{i-\frac{1}{2}}^{n+1}\right)\left(T_i^{n+1} - T_{i-1}^{n+1}\right)\right) -$$
$$- \rho_m\left(T_i^{n+1}\right) c_m\left(T_i^{n+1}\right)\left(T_i^{n+1} - T_i^n\right) = 0, \tag{30}$$

Let $U^s = (T_{i+1}^{s,n+1},\ T_i^{s,n+1}, T_{i-1}^{s,n+1})$, where s - iteration number. Then U^0 is an initial approximation of the system (30). After applying NEWTON's method for the system (30), the following approximation of the unknown grid function was obtained:

$$\begin{aligned}&\frac{\partial F(U^s)}{\partial T_{i+1}^{n+1}}(T_{i+1}^{s+1,n+1} - T_{i+1}^{s,n+1}) + \frac{\partial F(U^s)}{\partial T_i^{n+1}}(T_i^{s+1,n+1} - T_i^{s,n+1}) + \\ &+\frac{\partial F(U^s)}{\partial T_{i-1}^{n+1}}(T_{i-1}^{s+1,n+1} - T_{i-1}^{s,n+1}) + F(U^s) = 0,\end{aligned} \tag{31}$$

Expanding the brackets, the tridiagonal system will be given for (31):

$$A_i^s \left(T_{i+1}^{n+1}\right)^{s+1} + B_i^s \left(T_i^{n+1}\right)^{s+1} + C_i^s \left(T_{i-1}^{n+1}\right)^{s+1} = D_i^s, \tag{32}$$

where coefficients are equal:

$$\begin{aligned}&A_i^s = \frac{\partial F\left(U^s\right)}{\partial T_{i+1}^{n+1}},\ B_i^s = \frac{\partial F(U^s)}{\partial T_i^{n+1}},\ C_i^s = \frac{\partial F(U^s)}{\partial T_{i-1}^{n+1}}, \\ &D_i^s = -F\left(U^s\right) + A_i \left(T_{i+1}^{n+1}\right)^s + B_i \left(T_i^{n+1}\right)^s + C_i \left(T_{i-1}^{n+1}\right)^s.\end{aligned} \tag{33}$$

After expanding the equation (30), the corresponding derivatives are found:

$$\frac{\partial F\left(U\right)}{\partial T_{i+1}^{n+1}} = \frac{\Delta t}{(\Delta x)^2}\left(\frac{\partial k_m\left(T_{i+\frac{1}{2}}^{n+1}\right)}{\partial T_{i+1}^{n+1}} \cdot \left(T_{i+1}^{n+1} - T_i^{n+1}\right) + k_m\left(T_{i+\frac{1}{2}}^{n+1}\right)\right), \tag{34}$$

$$\begin{aligned}\frac{\partial F\left(U\right)}{\partial T_i^{n+1}} = &\frac{\Delta t}{(\Delta x)^2}\left(\frac{\partial k_m\left(T_{i+\frac{1}{2}}^{n+1}\right)}{\partial T_i^{n+1}} \cdot \left(T_{i+1}^{n+1} - T_i^{n+1}\right) - k_m\left(T_{i+\frac{1}{2}}^{n+1}\right)\right) - \\ &- \frac{\Delta t}{(\Delta x)^2}\left(\frac{\partial k_m\left(T_{i-\frac{1}{2}}^{n+1}\right)}{\partial T_i^{n+1}} \cdot \left(T_i^{n+1} - T_{i-1}^{n+1}\right) + k_m\left(T_{i-\frac{1}{2}}^{n+1}\right)\right) - \\ &- \frac{\partial c_m\left(T_i^{n+1}\right)}{\partial T_i^{n+1}}\rho_m\left(T_i^{n+1}\right)\left(T_i^{n+1} - T_i^n\right) - \\ &- \frac{\partial \rho_m\left(T_i^{n+1}\right)}{\partial T_i^{n+1}}c_m\left(T_i^{n+1}\right)\left(T_i^{n+1} - T_i^n\right) - \rho_m\left(T_i^{n+1}\right)c_m\left(T_i^{n+1}\right),\end{aligned} \tag{35}$$

$$\frac{\partial F\left(U\right)}{\partial T_{i-1}^{n+1}} = -\frac{\Delta t}{(\Delta x)^2}\left(\frac{\partial k_m\left(T_{i-\frac{1}{2}}^{n+1}\right)}{\partial T_{i-1}^{n+1}} \cdot \left(T_i^{n+1} - T_{i-1}^{n+1}\right) - k_m\left(T_{i-\frac{1}{2}}^{n+1}\right)\right), \tag{36}$$

Similarly, the boundary conditions will be disclosed. Taking into account the dependence of thermal conductivity and heat transfer coefficients on temperature, let us consider left boundary condition from (29) and rewrite it as:

$$H\left(T_0^{n+1}, T_1^{n+1}\right) \equiv k_m\left(T_{\frac{1}{2}}^{n+1}\right)\frac{T_1^{n+1} - T_0^{n+1}}{\Delta x}h_m(T_0^{n+1})\left(T_0^{n+1} - T_\infty^{L,n+1}\right) = 0. \tag{37}$$

Using NEWTON's method, the corresponding equation is found:

$$\begin{aligned}&\frac{\partial H(T_0^{n+1,s}, T_1^{n+1,s})}{\partial T_0^{n+1}}\left(T_0^{n+1,s+1} - T_0^{n+1,s}\right) + \frac{\partial H(T_0^{n+1,s}, T_1^{n+1,s})}{\partial T_1^{n+1}}\left(T_1^{n+1,s+1} - T_1^{n+1,s}\right) + \\ &+ H(T_0^{n+1,s}, T_1^{n+1,s}) = 0.\end{aligned} \tag{38}$$

Let's expand the derivatives:

$$\frac{\partial H(T_0^{n+1}, T_1^{n+1})}{\partial T_0^{n+1}} = \frac{k_m\left(T_{\frac{1}{2}}^{n+1}\right)}{\partial T_0^{n+1}} \cdot \frac{T_1^{n+1} - T_0^{n+1}}{\Delta x} - \frac{k_m\left(T_{\frac{1}{2}}^{n+1}\right)}{\Delta x} - \\ - \frac{\partial h_m\left(T_0^{n+1}\right)}{\partial T_0^{n+1}}\left(T_0^{n+1} - T_\infty^{L,n+1}\right) - h_m(T_0^{n+1}), \tag{39}$$

Similarly

$$\frac{\partial H(T_0^{n+1}, T_1^{n+1})}{\partial T_1^{n+1}} = \frac{k_m\left(T_{\frac{1}{2}}^{n+1}\right)}{\partial T_1^{n+1}} \cdot \frac{T_1^{n+1} - T_0^{n+1}}{\Delta x} + \frac{k_m\left(T_{\frac{1}{2}}^{n+1}\right)}{\Delta x}, \tag{40}$$

Using same procedures, you can apply NEWTON's method for the other boundary condition.

Taking linearized solution of discrete problem (28) as an initial iteration for NEWTON's method and using THOMAS' method to solve (32) - (40) one can find solution of the nonlinear problem.

4 Experimental design

(a) (b)

Figure 4. *Containers with different soils (a), container's backside with sensor cabels (b).*

The experimental facility is created and used to obtain the data for finding thermophysical properties of real soil. The setup is 3D printed a two-chamber container with interior measurements 30 cm × 12 cm × 10 cm, built with 1 cm thick thermal insulated walls. A picture of the experimental setup is shown in Figure 4. First chamber was filled with sand and the second with chernozem. Containers' front side is heated with lamps. In this research radiation from the lamps is neglected due to dominance of convective and conduction regimes at lower temperatures. The rear surface is influenced by the ambient temperature. The total sequence of experimental data corresponds to 10 days and the physical domain is defined for $x \in [0, \xi] \times [\xi, L]$ with $\xi = 15$ cm and $L = 30$ cm.

In case of sensors, two-chamber containter is monitored as shown in Figure 1. Two thermocouples (TC) are set on front and rear surfaces of the chamber. One sensor is set on the contact between two materials $x = \xi$ as illustrated on Figure 1. The position uncertainty is $\sigma_x = 0.5$ cm on the $x-$axis. The outside temperatures of air are measured with a sensor placed close to front and rear surfaces. Each sensor consecutively measure temperature every 10 min, which is illustrated in Figure 5.

The total uncertainty on the observations are evaluated through the propagation of the uncertainties. For the temperature, the total uncertainty is computed according to:

$$\sigma_T = \sqrt{\sigma_m^2 + \sigma_x^2 + \sigma_t^2}, \tag{41}$$

where $\sigma_m = 0.1$ °C is the measurement sensor uncertainty, σ_x is the uncertainty due to the sensor location and σ_t is the uncertainty due to the response time of the sensor. The last terms are given by:

$$\sigma_x = \frac{\partial T}{\partial x}\delta_x, \quad \sigma_t = \frac{\partial T}{\partial t}\delta_t, \tag{42}$$

where $\delta_x = 0.5$ cm and $\delta_t = 0.75$ s are position uncertainty and the response time of the sensor, respectively. The term $\frac{\partial T}{\partial x}$ in Eq.(42) is obtained at the location of the sensors using the numerical solution. In case of ambient air this term is omitted. The second term $\frac{\partial T}{\partial t}$ is computed using the measurements and a discrete second order finite difference scheme. The uncertainty of the measurements compared to estimated temperature are shown in Figure 6 and Figure 9 in the gray shadows.

The temperature at $t = 0$ is assumed to be interpolation of measured temperature. Thus, first order polynomials of $x \in [0, L]$ are fitted for each chamber of the container.

$$T^0(x) = \begin{cases} \frac{(Y_\xi^0 - Y_0^0)\cdot x}{L} + Y_0^0, & x \in [0, \xi], \\ \frac{(Y_L^0 - Y_\xi^0)\cdot x}{L} + Y_\xi^0, & x \in [\xi, L]. \end{cases} \tag{43}$$

These interpolation functions are used as initial conditions for numerical solution.

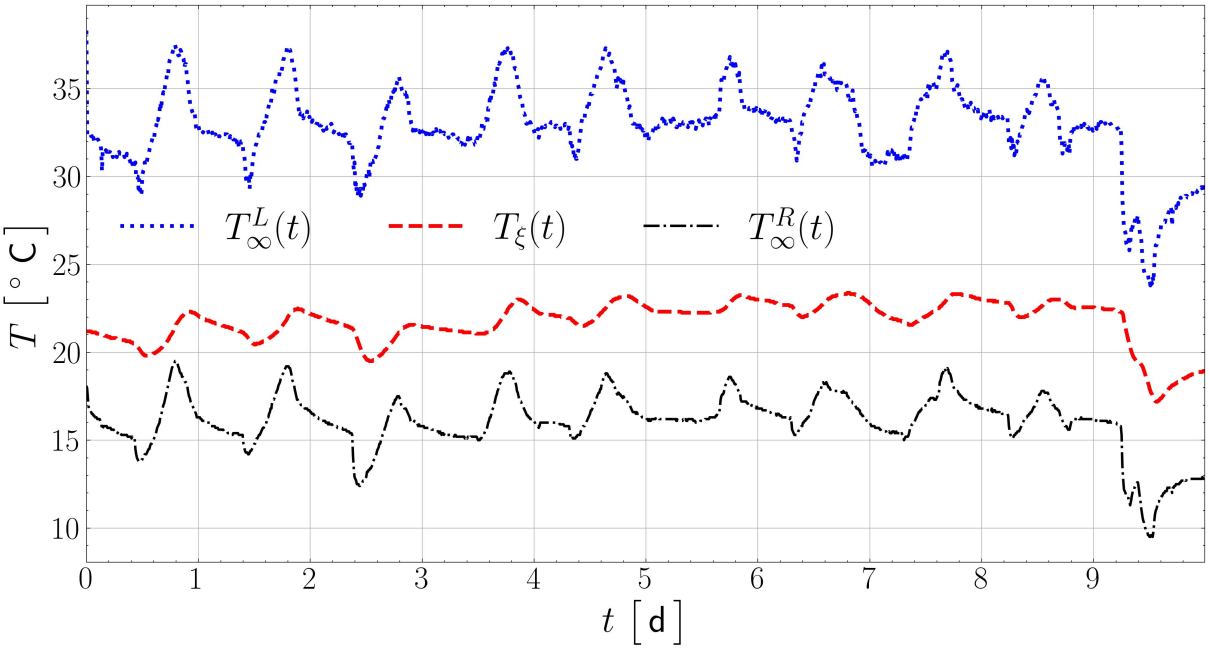

Figure 5. *Measurement time variations of the left and the right ambient temperatures and the temperature at* $x = \xi$.

5 Results and discussion

The thermophysical properties estimation problem is solved using the algorithm described in Section 2.4. The time and space steps are $\Delta t = 10$ min and $\Delta x = 3.75 \times 10^{-4}$ m. The a

Table 1. *The a initial and estimated values of the first material parameters*

	$k_{1,0}$	$k_{1,1}$	$k_{1,2}$	$k_{1,3}$	$c_{1,0}$	$c_{1,1}$	$\rho_{1,0}$	$\rho_{1,1}$	$h_{1,0}$	$h_{1,1}$
a priori values	0.33	0	0	0	0.19	0	1520	0	5	0
Estimated values	0.2313	$1.4 \cdot 10^{-4}$	$9.5 \cdot 10^{-5}$	$-1.1 \cdot 10^{-6}$	0.1782	0.0014	1413	3.1713	4.6896	0.0338

Table 2. *The initial and estimated values of the second material parameters*

	$k_{2,0}$	$k_{2,1}$	$k_{2,2}$	$k_{2,3}$	$c_{2,0}$	$c_{2,1}$	$\rho_{2,0}$	$\rho_{2,1}$	$h_{2,0}$	$h_{2,1}$
a priori values	0.6	0	0	0	0.2	0	1600	0	5	0
Estimated values	0.6359	$8.3 \cdot 10^{-5}$	$1.1 \cdot 10^{-4}$	$-1.2 \cdot 10^{-6}$	0.1794	0.0021	1511	2.9314	4.9048	0.0375

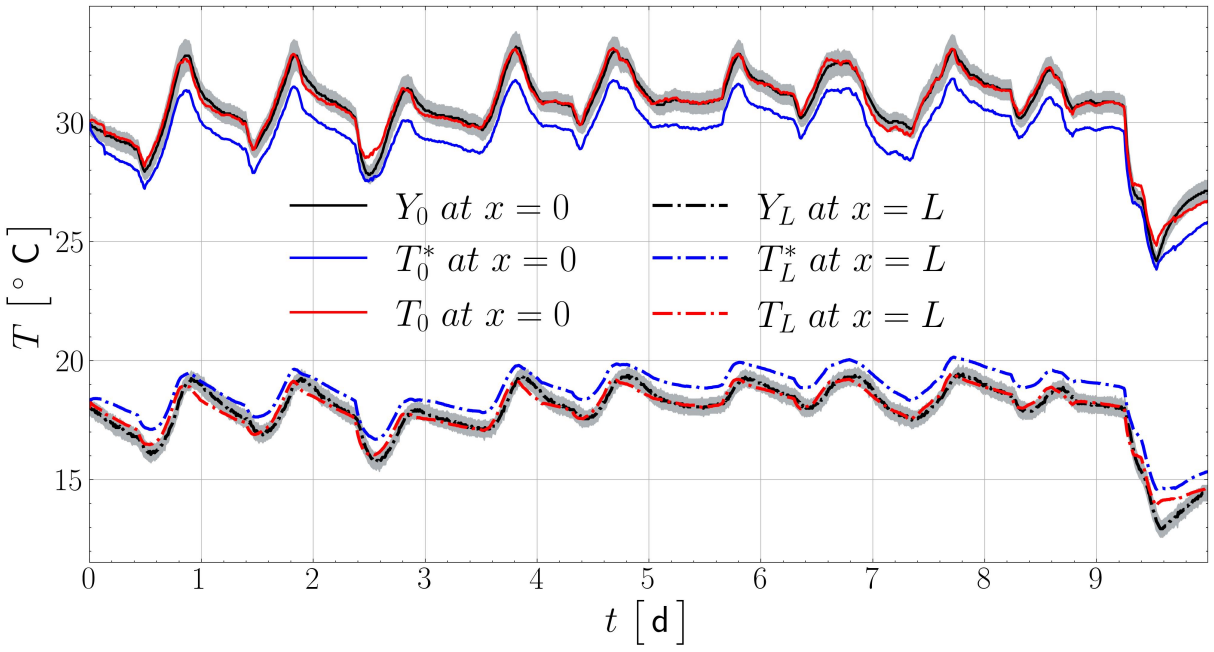

Figure 6. *Variation of the temperature from experimental observations* (Y_0, Y_L)*, the temperature with a priori material properties* (T_0^*, T_L^*) *and the estimated temperature* (T_0, T_L) *at* $x^* = 0$ *and* $x^* = L$*.*

Table 3. *Correlation between the sensitivity coefficients for heat conductivity parameters of two materials.*

	$k_{1,0}$	$k_{1,1}$	$k_{1,2}$	$k_{1,3}$
$k_{1,0}$	1	−0.93	−0.94	0.92
$k_{1,1}$	–	1	0.83	−0.81
$k_{1,2}$	–	–	1	−0.86
$k_{1,3}$	–	–	–	1

	$k_{2,0}$	$k_{2,1}$	$k_{2,2}$	$k_{2,3}$
$k_{2,0}$	1	−0.92	−0.69	0.88
$k_{2,1}$	–	1	0.81	−0.87
$k_{2,2}$	–	–	1	−0.79
$k_{2,3}$	–	–	–	1

priori material properties are given from table values from Tables 1 and 2. The reliability of the *a priori* values are well established in [31]. Then, the parameter estimation problem is solved

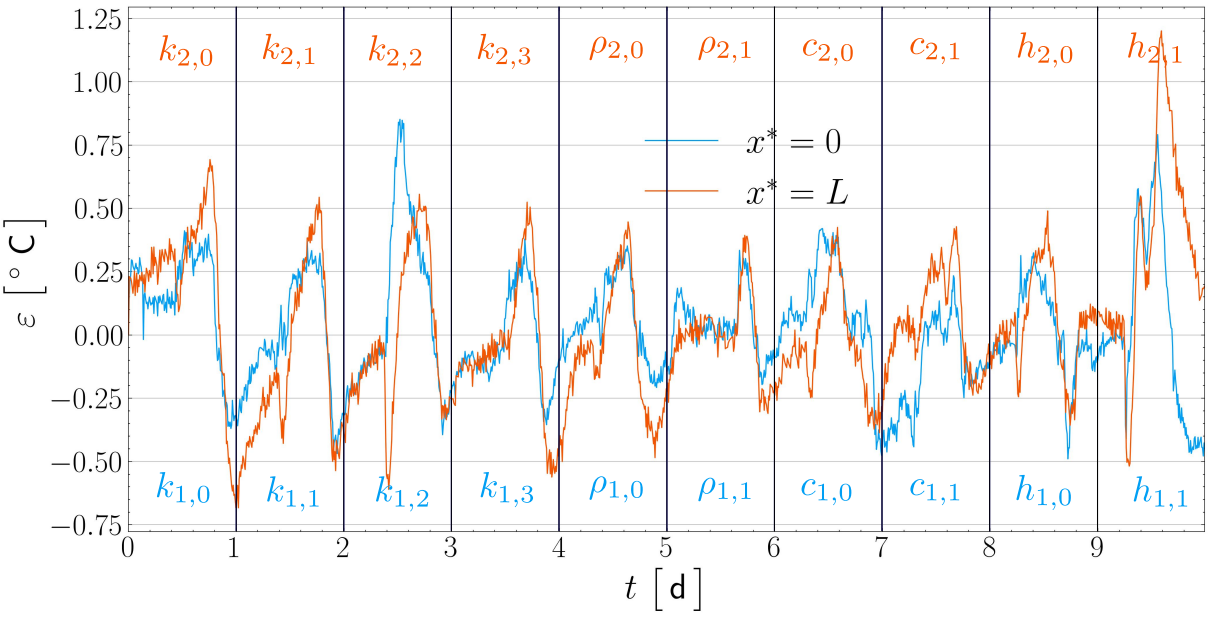

Figure 7. *Variation of the error between estimated and experimental observation temperatures* $\varepsilon = Y^n_{x^*} - T^n_{x^*}$ *at* $x^* = 0$ *and* $x^* = L$.

Table 4. *Correlation between the sensitivity coefficients.*

(a) *Same container*

	$k_{1,0}$	$c_{1,0}$
$k_{1,0}$	1	0.79
$c_{1,0}$	–	1

(b) *Different containers*

	$k_{1,0}$	$k_{2,0}$
$k_{1,0}$	1	0.87
$k_{2,0}$	–	1

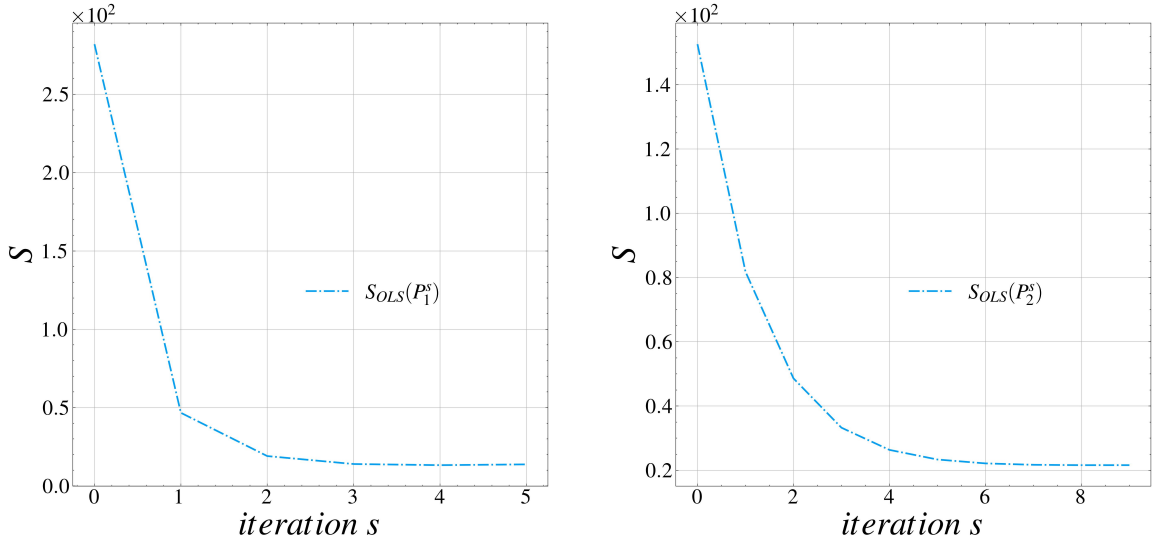

Figure 8. *The variation of the objective function with respect to iteration for the first (a) and the second (b) materials.*

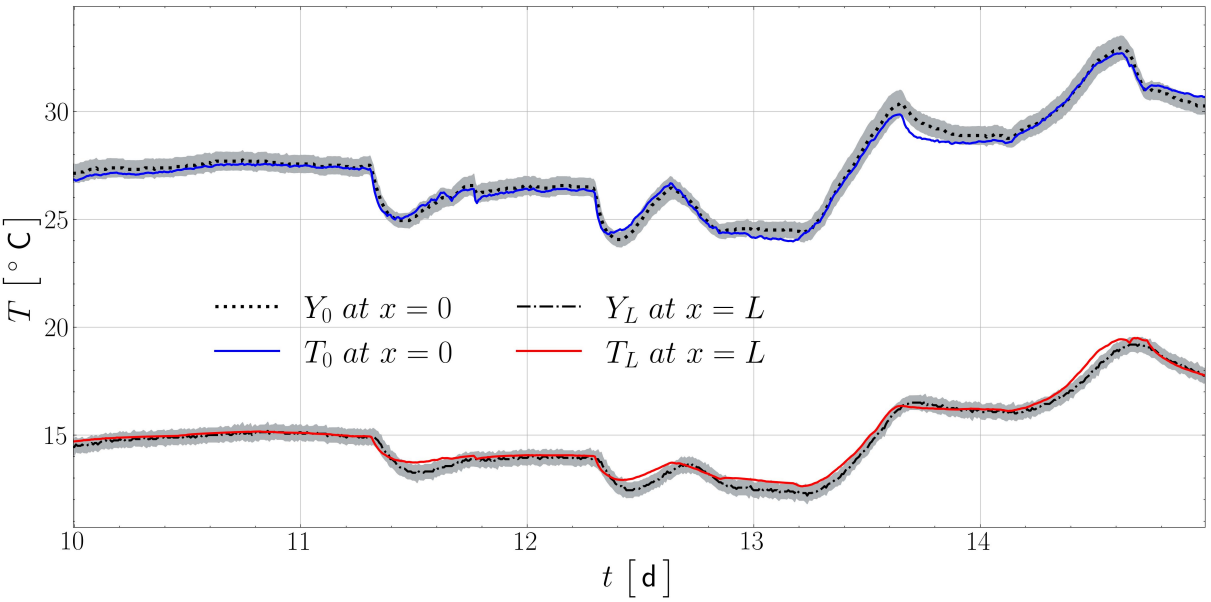

Figure 9. *Comparison of the experimental observations* (Y_0, Y_L) *and the temperature with estimated parameters* (T_0, T_L) *at* $x^* = 0$ *and* $x^* = L$ *for the additional 5 days.*

considering the ten days of experiments. The obtained estimated results are reported in the Tables 1 and 2. The value of the parameter is in accordance with the physical expectations.

The results from direct problem are then compared to the experimental observation data. The respective measurements with uncertainty boundaries in two sensor locations $x^* = 0$ and $x^* = L$ and the temperature for *a priori* and estimated values from the direct problem are illustrated in Figure 6. The estimation values were in satisfactory agreement for all points of observations unlike *a priori* values. The discrepancy between numerical predictions and observations remains in the uncertainty band of the measurements. At last day of observations there are some little discrepancies for the temperature at $x^* = L$. The residual error between the observations and the numerical results are given in Figure 7 for the temperature at different sensor locations respectively. As expected residuals are higher at the end of the experiments $t \in [9, 10]$ d, which indicate that some physical phenomena may be omitted in the mathematical model, particularly during the sharp/quick increase in temperature.

The calculation of the sensitivity equations are realised using the numerical problems (24)-(27) described in Section 2.3. The space and time discretization are the same as in the direct problem. It is important to remark that the twenty parameters are theoretically identifiable because the experimental design enables to obtain two observable experimental data at the boundaries. First field divided to ten time intervals for the ten unknown parameters from first material and second field in the same way divided for other ten unknown parameters for second material. Without these constrictions for calculation time intervals for each parameter, the theoretical identifiability could not be demonstrated.

The correlation between the sensitivity coefficients for some parameters which are calculated in the same time interval are given in Tables 3 and 4. Thus due to linear dependency of parameters it is impossible to calculate parameters in the same time intervals. The correlation between unknown parameters is reduced by using different observation time steps and different sensor locations for each coefficient like it was mentioned before. From practical point of view all the unknown parameters are identifiable.

Figure 8 illustrates the variation of the objective function with respect to iteration from the initial step until the convergence point of the criteria (22). Less than 10 iterations are required for the algorithm to estimate the parameters. This is achieved due to steepest gradient

property of LEVENBERG-MARQUARDT method for parameter estimation in (18). In addition, the computational time of the direct problem also fast thanks to the convergence of the NEWTON's method. It is important to note that *a priori* values for the unknown parameters and for the temperature in NEWTON's method is crucial for the fast convergence. The regularization parameter α from Eq. 11 which is found from L-curve is equal to 0.01. Figure 2 illustrates a tradeoff-curve between temperature and parameters residuals. It can be seen that if too much regularization or damping is imposed on the solution, then temperature residual will be too large. On the other hand, if too little regularization is imposed, then the solution will be dominated by the contributions from the data errors, hence parameter residual will be too large.

Last, the reliability of the model is evaluated. For this, the numerical predictions of the model are compared against an extra-set of measurement data (not used to get the inverse problem solution). The experimental data for the next five days $t \in (10, 15]$ d are used. Figure 9 shows the comparison of temperature using estimated thermophysical parameters with experimental data. A very satisfying agreement is observed between the numerical predictions and the observations, validating the reliability of the calibrated model.

6 Conclusion

The knowledge of the soil thermophysical properties is an important part of the assessment of soil energy balance. This article is concerned with the estimation of these parameters such as the thermal conductivity, the heat specific heat capacity, density and heat transfer coefficients of two different materials, which are sand and chernozem. These parameters are assumed as nonlinear, *i.e.* varying with the temperature field. Real experiment was conducted, a two-chamber container was constructed to obtain experimental data. It was monitored by five sensors: two were placed on the rear ends of the container, two close to the rear ends to measure ambient temperature and one located at the border of two soil materials. The experimental set up is carried out during fifteen days. One side of the container is exposed to heat. Ten days data are used to estimate unknown parameters and five days data are used to evaluate the reliability of the model. The nonlinear direct problem was solved with finite-difference by using an implicit discretization in time. The NEWTON's method is used to solve nonlinear problem. The LEVENBERG-MARQUARDT method is employed to solve the parameter estimation problem and minimized the least square estimator with TIKHONOV's regularization. Selection of the regularization parameter is made through L-curve technique, which helped to alleviate instabilities on the solution of the ill-posed nature of the inverse problem. Proper use of regularization parameter allowed us to avoid oscillations of the solution and increase a speed of the convergence of the objective function. The sensitivity coefficients are computed by derivative-based approach with direct differentiation of the governing equations which leads to solution additional sensitivity equations for all parameters. It provides an accurate and continuous time-varying sensitivity coefficients. The results highlight that the algorithm is efficient and fast to obtain the solution of the inverse heat conduction problem. The estimated parameters are in accordance with *a priori* values. Last, the experimental data for the first 10 days $t \in [0, 9]$ d is used to solve inverse problem and for the reliability the experimental data for next 5 days $t \in [10, 15]$ d is used. The reliability of the calibrated model is satisfying with a discrepancy between numerical predictions and experimental observations remaining within the measurement error. Described method allows nondestructive practical application for estimation of thermophysical properties in real field problems. Further research should focus on extending the methodology for more complex physical models including, coupled heat and mass transfer in porous materials and implementation of the algorithm in real field conditions.

Acknowledgements

The work is supported by grant funding for projects of the Ministry of Education and Science of the Republic of Kazakhstan (Grant AP19677594).

References

[1] Lyesse Laloui and Alessandro F. Rotta Loria. Chapter 2 - energy geostructures. In Lyesse Laloui and Alessandro F. Rotta Loria, editors, *Analysis and Design of Energy Geostructures*, pages 25–65. Academic Press, 2020. 1

[2] Samuel C. Johnson, F. Todd Davidson, Joshua D. Rhodes, Justin L. Coleman, Shannon M. Bragg-Sitton, Eric J. Dufek, and Michael E. Webber. Chapter five - selecting favorable energy storage technologies for nuclear power. In Hitesh Bindra and Shripad Revankar, editors, *Storage and Hybridization of Nuclear Energy*, pages 119–175. Academic Press, 2019. 1

[3] Shafagh Ida, Paul Shepley, Will Shepherd, and Fleur Loveridge. Thermal energy transfer around buried pipe infrastructure. *Geomechanics for Energy and the Environment*, 29:100273, 2022. 1

[4] Pierre Delage, Y.J. Cui, and A.M. Tang. Clays in radioactive waste disposal. *Journal of Rock Mechanics and Geotechnical Engineering*, 2(2):111–123, 2010. 1

[5] Fattahi Morteza. Possible soil thermal response to seismic activities in alborz region (iran). *Nat. Hazards Earth Syst. Sci.*, page 459–464, 2010. 2

[6] Paul Lunt, Kate Fuller, Matthew Fox, Steve Goodhew, and Thomas Murphy. Comparing the thermal conductivity of three artificial soils under differing moisture and density conditions for use in green infrastructure. *Soil Use and Management*, n/a(n/a). 2

[7] Wen Haiyan, Jun Bi, and Ding Guo. Calculation of the thermal conductivities of fine-textured soils based on multiple linear regression (mlr) and artificial neural networks (ann). *European Journal of Soil Science*, 71, 01 2020. 2

[8] Hailong He, Kosuke Noborio, Øistein Johansen, Miles Dyck, and Jialong Lv. Normalized concept for modelling effective soil thermal conductivity from dryness to saturation. *European Journal of Soil Science*, 71(1):27–43, 2020. 2

[9] Bing Tong, Dilia Kool, Joshua Heitman, Thomas Sauer, Zhiqiu Gao, and Robert Horton. Thermal property values of a central iowa soil as functions of soil water content and bulk density or of soil air content. *European Journal of Soil Science*, 71(2):169–178, 2020. 2

[10] Si Hong Wu and Per-Erik Jansson. Modelling temperature, moisture and surface heat balance in bare soil under seasonal frost conditions in china. *European Journal of Soil Science*, 62(6):780–796, 2011. 2

[11] Yili Lu, Robert Horton, and Tusheng Ren. Simultaneous determination of soil bulk density and water content: a heat pulse-based method. *European Journal of Soil Science*, 69(5):947–952, 2018.

[12] Jarkko Okkonen, Pertto Ala-Aho, and Pekka Hänninen. Multi-year simulation and model calibration of soil moisture and temperature profiles in till soil. *European Journal of Soil Science*, 68(6):829–839, 2017. 2

[13] M.N. Ozisik and H.R.B. Orlande. *Inverse Heat Transfer - Fundamentals and Applications*. CRC Press, New York, 2000. 2

[14] A.N. Tikhonov, A. Goncharsky, V.V. Stepanov, and A.G. Yagola. *Numerical Methods for the Solution of Ill-Posed Problems*. Mathematics and Its Applications. Springer Netherlands, 2013. 2, 5

[15] A. N. Tikhonov. Solution of incorrectly formulated problems and the regularization method. *Soviet Math. Dokl.*, 4:1035–1038, 1963. 2

[16] A. N. Tikhonov. Inverse problems in heat conduction. *Journal of engineering physics*, 29:105433, 1975. 2, 5

[17] O. M. Alifanov. Identification of heat transfer processes in flying vehi- cles. *Introduction to the Theory of Inverse Heat Transfer Problems, Mashinostroe- nie*, 1994. 2

[18] O. M. Alifanov. *Inverse Heat Transfer Problems*. Springer New York, NY, 1994.

[19] O. Alifanov, E. Artyukhin, and S. Rumyantsev. *Extreme Methods for Solving Ill-Posed Problems with Applications to Inverse Heat Transfer Problems*. 04 2015. 2

[20] James V. Beck and Keith A. Woodbury. Inverse problems and parameter estimation: integration of measurements and analysis. *Measurement Science and Technology*, 9(6):839, 1998. 2

[21] Erkki Somersalot Jari P. Kaipio. *Statistical and Computational Inverse Problems*. Springer New York, NY, 2004. 2

[22] Phan Xuan Thanh. Space-time finite element method for determination of a source in parabolic equations from boundary observations. *Journal of Inverse and Ill-Posed Problems*, 29(5):689 – 705, 2021. Cited by: 1. 2

[23] Kian Tafazzoli Aghvami, Mohammad Hassan Shojaeefard, and Mahmoud Jourabian. Steady-state estimation of thermal contact conductance between sliding disk and stationary cylinder with similar/dissimilar materials under the isothermally heated boundary condition. *Heat Transfer*, 50(8):8012 – 8034, 2021. Cited by: 0.

[24] Talaat Abdelhamid, Rongliang Chen, and Mahbub Alam. Prediction of multi-parameters in the inverse heat conduction problems. volume 1707, 2020. Cited by: 2; All Open Access, Gold Open Access. 2

[25] Farzad Mohebbi, Ben Evans, and Timon Rabczuk. Solving direct and inverse heat conduction problems in functionally graded materials using an accurate and robust numerical method. *International Journal of Thermal Sciences*, 159, 2021. Cited by: 5; All Open Access, Green Open Access. 2

[26] Tao Min, Xing Chen, Yao Sun, and Qiang Huang. A numerical approach to solving an inverse heat conduction problem using the levenberg-marquardt algorithm. In Suvanjan Bhattacharya, Mohammad Moghimi Ardekani, Ranjib Biswas, and R. C. Mehta, editors, *Inverse Heat Conduction and Heat Exchangers*, chapter 6. IntechOpen, Rijeka, 2019. 2

[27] Miao Cui, Kai Yang, Xiao liang Xu, Sheng dong Wang, and Xiao wei Gao. A modified levenberg–marquardt algorithm for simultaneous estimation of multi-parameters of boundary heat flux by solving transient nonlinear inverse heat conduction problems. *International Journal of Heat and Mass Transfer*, 97:908–916, 2016.

[28] Miao Cui, Yi Zhao, Bingbing Xu, and Xiao wei Gao. A new approach for determining damping factors in levenberg-marquardt algorithm for solving an inverse heat conduction problem. *International Journal of Heat and Mass Transfer*, 107:747–754, 2017.

[29] Ramin Sajedi, Javad Faraji, and Farshad Kowsary. A new damping strategy of levenberg-marquardt algorithm with a fuzzy method for inverse heat transfer problem parameter estimation. *International Communications in Heat and Mass Transfer*, 126:105433, 2021. 2

[30] V. A. Morozov. *Methods for Solving Incorrectly Posed Problems*. Springer New York, NY, 1984. 5

[31] S Acherkan N. *Spravochnik mashinostroitelya*. 1956, 1956. 13